



OPEN

SUBJECT AREAS:

PRE-CLINICAL STUDIES
BIOMEDICAL ENGINEERING
ANATOMYReceived
24 September 2013Accepted
17 December 2013Published
14 January 2014Correspondence and
requests for materials
should be addressed to
M.D. (martin.
donnelley@adelaide.
edu.au)

Non-invasive airway health assessment: Synchrotron imaging reveals effects of rehydrating treatments on mucociliary transit in-vivo

Martin Donnelley^{1,2,3}, Kaye S. Morgan⁴, Karen K. W. Siu^{4,5,6}, Nigel R. Farrow^{1,2,3}, Charlene S. Stahr⁷, Richard C. Boucher⁸, Andreas Fouras⁷ & David W. Parsons^{1,2,3}

¹Respiratory and Sleep Medicine, Women's and Children's Hospital, 72 King William Road, North Adelaide, SA, 5006, Australia, ²Centre for Stem Cell Research, University of Adelaide, SA, 5001, Australia, ³School of Paediatrics and Reproductive Health, University of Adelaide, SA, 5001, Australia, ⁴School of Physics, Monash University, Clayton, Vic, 3800, Australia, ⁵Monash Biomedical Imaging, Monash University, Clayton, Vic, 3800, Australia, ⁶Imaging and Medical Beamline, Australian Synchrotron, Clayton, Vic, 3800, Australia, ⁷Mechanical and Aerospace Engineering, Monash University, Clayton, Vic, 3800, Australia, ⁸CF/Pulmonary Research & Treatment Center, The University of North Carolina at Chapel Hill, Chapel Hill, North Carolina, USA.

To determine the efficacy of potential cystic fibrosis (CF) therapies we have developed a novel mucociliary transit (MCT) measurement that uses synchrotron phase contrast X-ray imaging (PCXI) to non-invasively measure the transit rate of individual micron-sized particles deposited into the airways of live mice. The aim of this study was to image changes in MCT produced by a rehydrating treatment based on hypertonic saline (HS), a current CF clinical treatment. Live mice received HS containing a long acting epithelial sodium channel blocker (P308); isotonic saline; or no treatment, using a nebuliser integrated within a small-animal ventilator circuit. Marker particle motion was tracked for 20 minutes using PCXI. There were statistically significant increases in MCT in the isotonic and HS-P308 groups. The ability to quantify *in vivo* changes in MCT may have utility in pre-clinical research studies designed to bring new genetic and pharmaceutical treatments for respiratory diseases into clinical trials.

Mucociliary transport (MCT) requires the coordinated beating of cilia, microscopic hair-like structures, to propel the airway surface liquid (ASL) across the surfaces of epithelial cells. This integrated activity provides the primary method for removing deposited pathogens and particulates from airway surfaces. In cystic fibrosis (CF), a dysfunctional CF transmembrane conductance regulator (CFTR) ion channel in airway epithelial cells results in dehydration of the ASL and impaired MCT. The MCT failure produces retention of inhaled pathogens and particulates, mucus obstruction, chronic infection, and eventually lung failure¹. Current clinical assessments of CF airway disease and its treatment are indirect. A logical method to assess the effect of CF treatments on airway surfaces is to directly measure restoration of MCT activity by tracking the movement of deposited marker particles along the airways. The ability to directly visualise deposited particle MCT behaviour in live animal model airways could provide spatio-temporal information pertaining to the initiation and maintenance of CF pathophysiology and potentially reveal novel directions for the development of preventative therapies for CF airway disease.

To determine the efficacy of genetic^{2,3} and other potential therapies for CF airway disease in animal models, with a view to ultimate use in humans, we have developed a novel MCT monitoring method based on measuring the transit rate and behaviour of individual particles deposited in the lungs using synchrotron phase contrast X-ray imaging (PCXI). This technique can be used *in vivo* in live anaesthetised mice⁴⁻⁶. By comparison, conventional *in vivo* MCT measurement methods rely on measuring bulk particle clearance from the airways⁷⁻¹⁰, are unable to track the motion of *individual* micron sized deposited particles with high spatial or temporal resolution, and cannot be used to assess spatial or temporal variations in MCT homogeneity within the airways.

An alternative method to accurately track individual particle MCT involves the use of an *ex vivo* system. A recent study examined the transit of individual deposited particles of dried ink in an *ex vivo* porcine system, and determined that MCT on untreated airways was ~4 mm/min and varied with treatment¹¹. Similarly, Ballard et al.¹²



showed that treatment with hypertonic saline restored MCT in only half of the *ex vivo* porcine tracheas they tested, but that surface active substances provided additional benefits in restoration of MCT. However, the obvious limitation of these systems is the requirement for tissue excision and support in an artificial environment. We propose that direct, non-invasive visualisation of individual deposited particle MCT in live intact animal-model airways should: (1) improve our understanding of airway health and disease and (2) allow the effects of therapeutic agents on MCT to be rapidly and accurately quantified.

PCXI can produce enhanced soft tissue contrast even when the absorption differences are small by utilising X-ray refraction in addition to conventional absorption. Provided the X-ray beam is spatially coherent, increasing the sample to detector distance^{13–15} enhances tissue boundaries due to the phase changes that are induced by differences in the tissue X-ray refractive indices. We have reported on the benefits of PCXI for non-invasive airspace imaging in small animals¹⁶, for non-invasive particulate detection in live mouse airways^{4–6,17}, and for the visualisation and assessment of surrogate fluid dosing regimes for airway gene therapy treatments in live mice^{18,19}. Our previous studies also examined the MCT behaviour of a range of common pollutant particles delivered to the airways in either a saline carrier fluid^{5,6} or as a dry powder⁴. These studies revealed that deposited lead dust, typically ranging from 5 μm up to 12 μm diameter and with a small number of larger particles present (see Figure 3 in Donnelley, Siu, et al.⁵), was a suitable marker for analysing tracheal MCT behaviour via PCXI. Furthermore, this technique also permits long-term repeated-measure study designs to assess treatments without animal sacrifice.

The aims of this study were to non-invasively observe the basal surface mucus transport activity of live mouse airways, at micron resolution, and to image and quantify changes in particle MCT produced by a rehydrating treatment for CF airways disease, i.e. inhaled hypertonic saline (HS) combined with a long acting epithelial sodium channel (ENaC) blocker (P308). HS acutely increases MCT in both CF and normal patients by directly increasing the osmotic load on the airway surface and triggering a water flux onto the airway surface. In CF this response can help rehydrate the airway surface and improve airway clearance²⁰. The ENaC channel is up-regulated in CF and further increases the ASL dehydration produced by the CFTR dysfunction, so any compound that inhibits the action of the ENaC channel should increase epithelial hydration. In this

study the combined HS-P308 treatment was used to maximise this rehydration effect, thereby producing a large change in MCT. Although the effects of rehydrating treatments such as HS on MCT have previously been observed in excised sections of airway epithelium¹², they have never been examined or quantified in intact airways *in vivo*.

Results

Experiments were performed at the SPring-8 synchrotron radiation facility in Japan. Lead marker particles were delivered to the airways of live anaesthetized and intubated mice, prior to PCXI. Mice ($n = 5$ per group) were randomly assigned to a no treatment control group, an isotonic saline aerosol control group, or the HS-P308 aerosol treatment group. Images were captured prior to, during and after aerosol delivery, and all particle movement was tracked to determine the MCT rate.

Assessment of the MCT rate of a large number of particles was chosen as a reliable indicator of the immediate effectiveness of isotonic saline or HS-P308 to alter airway MCT rates. For the 12 animals successfully studied (aerosol delivery failed in one animal from the isotonic group, and two from the HS-P308 group), the mean time between dry particle insufflation and initiation of the imaging run was 5 minutes. Deposited lead particles were immediately visible in the trachea of all animals when imaging began, but the majority were stationary for the first two imaging periods (i.e. during baseline, prior to aerosol delivery). The MCT rate rapidly increased within the aerosol delivery period. However, the particle transit was heterogeneous: that is, some particles did not move while others transited the field of view rapidly. In addition, as previously reported^{4–6}, many particles followed unpredictable and non-linear paths along the airway. An example of this motion is shown in Figure 3 and in the Supplementary Video.

A total of 11,743 individual particle MCT measurements were made for the 12 mice in the study. Figure 4 shows that the MCT rate was increased in the isotonic saline and HS-P308 treatment groups compared to the No Rx Control group at all post delivery time points. The MCT rate of the No Rx Control group was 0.27 ± 0.11 mm/min. Isotonic saline produced a more pronounced early (5.5 min) effect than HS-308, but the effect of HS-P308 was sustained and greater in magnitude at the later time points. Specifically, at the 5.5 min time-point the isotonic MCT rate was statistically higher than the HS-P308 group, whereas at the 13.5 min time-point the HS-P308 MCT

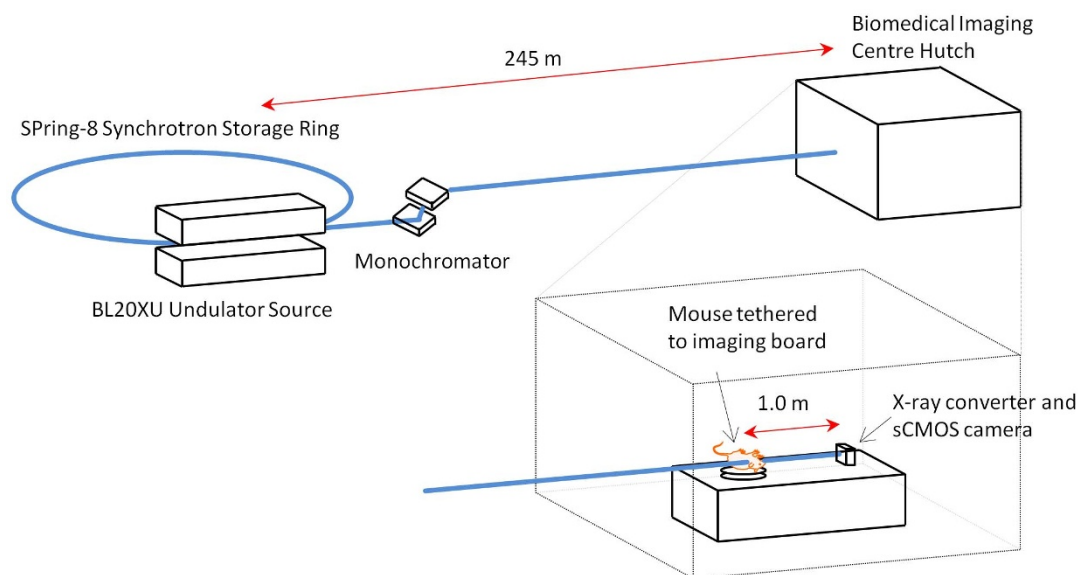


Figure 1 | The synchrotron *in vivo* PCXI setup. Mice are held supine on an x-y-rotation stage in the BL20XU imaging hutch, 245 m from the undulator X-ray source. A propagation distance of 1 m was used.

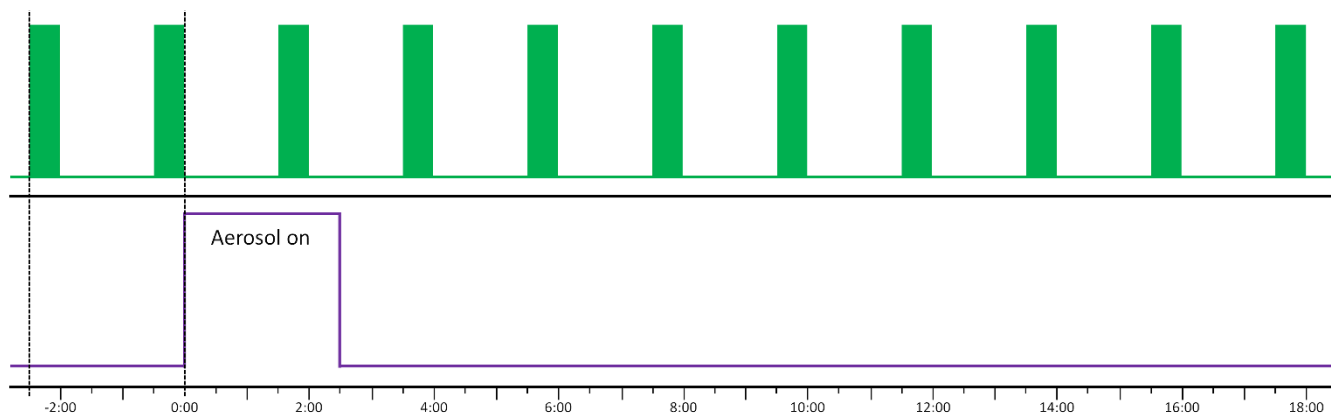


Figure 2 | The experimental imaging plan. Images were acquired in 30 second blocks (green bars, top panel) every two minutes at a rate of one image per breath (2 Hz). After two baseline imaging periods the aerosol (purple, lower panel) was delivered for 2.5 min. Imaging continued for a further ~18 minutes.

rate was significantly higher than the isotonic group. A total of 335 particles (i.e. <3% of the total number of particles tracked) were excluded from the analysis based on the chosen maximum-speed criteria, with a significantly greater number of particles excluded from the HS-P308 group than the isotonic group ($P < 0.05$, unpaired t-test). These results show that delivery of aerosolised fluid increased the MCT rate compared to control/baseline, regardless of the tonicity of the fluid. However, the initiation and duration of MCT effects after aerosol treatment differed with treatment.

The complex airway surface MCT particle movements are difficult to adequately describe and difficult to represent in static images (See Fig. 3), so the Supplementary Video should be viewed to reveal the nature of particle movements and to enable dynamic visual comparison of the effects of the isotonic saline and HS-P308 aerosols with the control group. The rapid onset of the effects of isotonic saline and the durable effect of HS-P308 are clearly visible in this comparison

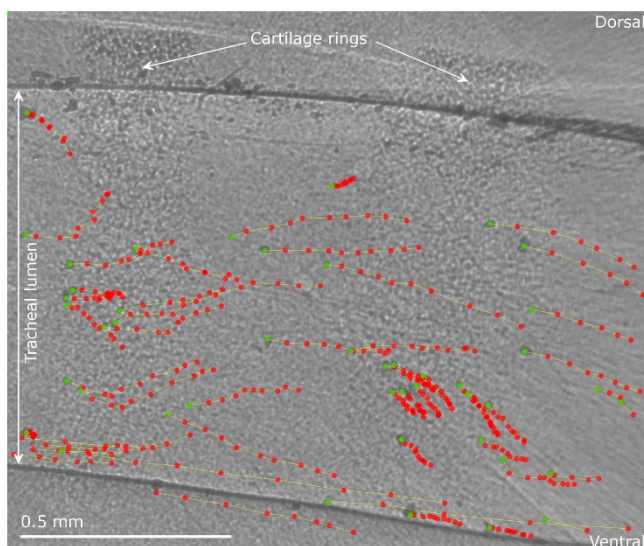


Figure 3 | Typical PCXI image showing the result from manual particle tracking at one imaging period. The mouse is supine with the lungs to the left and the mouth to the right; MCT is primarily in a left-to-right direction. The first frame (marked in green) from a sequence of 10 is shown with the location of tracked particles in the following frames marked with a red dot. Note that particle motion is not homogeneous; some particles move long distances, some short distances, and some (unmarked, primarily along the dorsal tracheal surface) remain stationary over those 10 frames.

video. Note that in these X-ray image sequences all particle activities on both (lateral) tracheal walls are superimposed, so it is not possible to determine which tracheal wall surface (i.e. the near or the far wall) the particulates are located on. In addition, some particulates and particulate motion appears to be located below the apparent tracheal edge. As previously reported⁴, this phenomenon is due to the ω shaped dorsal wall of the trachea formed by an epithelial protrusion in the dorsal surface of the trachea into the lumen.

Discussion

This study has demonstrated that aerosolised fluid increased the mean MCT rate of individual particles deposited onto the tracheal airway surface compared to a control group, and that HS-P308, a CF airway-hydrating therapy, produced a more sustained increase in MCT rate compared to isotonic saline. Importantly, these findings show for the first time that it is possible to directly compare the effects of pharmaceutical treatments on individual particle MCT in mice *in vivo*.

The basal rates of transit measured in this study were lower than those reported by Grubb *et al.*⁷ who used a dye-transit technique and reported that bulk mouse tracheal MCT was 2.2 ± 0.45 (SE) mm/min. Via comparisons to other studies, Grubb *et al.* also noted that the recorded MCT rate was heavily influenced by the marker size/type used. The lead particles used in the present study may be

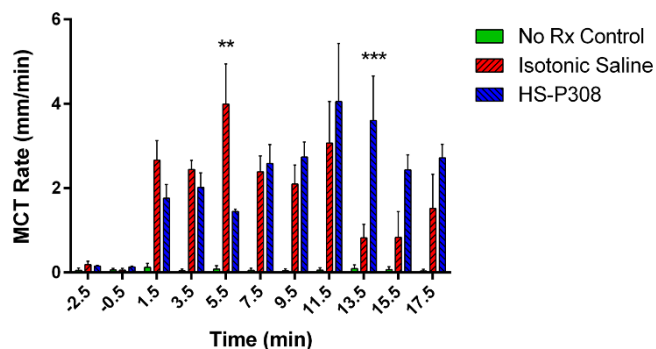


Figure 4 | Effect of therapeutics on MCT. The MCT rate was calculated by manually tracking the movement of up to 50 particles across 10 frames at each time point in each mouse. MCT rates are presented as mean and standard error of the mean ($\bar{x} \pm SE$). Statistical significance was set at $p = 0.05$ and power = 0.80 and MCT rates were analysed by two way RM-ANOVA with Bonferroni multiple comparisons. The difference in MCT rate between the Isotonic and HS-P308 group at the 5.5 and 13.5 min time points was statistically significant (** $p < 0.01$ and *** $p < 0.001$).



handled by the MCT system in a different manner to either fluorescent dyes⁷ or ink particles¹¹, both of which are much smaller and lighter. However, in a previous lead marker particle study we recorded a tracheal MCT rate of 1.82 ± 1.6 mm/min⁴, a rate that was substantially higher than what we recorded in this study. We hypothesise that the absence of an inspiratory humidification system in this study may have resulted in dehydration of the airway surface by the dry imaging hutch air used to ventilate the animals, resulting in slower baseline and control MCT rates.

The effects of isotonic saline on accelerating MCT were rapid, i.e., peaked at 5.5 min, but were short-lived. We speculate that the initial, rapid effect was mediated by rehydrating the ventilator-induced dehydrated airway surface, with restoration of MCT. However, the effect of isotonic saline was relatively short lived because the added volume was rapidly absorbed by the epithelium by an ENaC mediated Na⁺ absorption mechanism^{21,22}. In contrast, the effect of HS-P308 on MCT exhibited the opposite pattern, i.e., a moderate early effect (5.5 min) with a more robust delayed (15.5 min) response. Two possible explanations could account for the moderation of the early response. First, it has been reported that amiloride blocks aquaporin mediated transepithelial water flow in response to imposed osmotic gradients²³. However, the newer and more highly potent ENaC blockers, such as P308, do not appear to exhibit an aquaporin block activity²⁴. Second, it has been reported that rapid delivery of HS can overwhelm the ability of transepithelial water flow to buffer ASL hypertonicity following rapid aerosolization of HS²⁵. The consequence is loss of water from epithelial cells into the lumen, cell shrinkage, reduction in ciliary beat frequency, and slowed MCT. Although we favour the latter explanation, studies of HS vs. P308 alone will be required to rigorously test this possibility. With respect to the larger “delayed” increase in MCT following HS-P308 vs. isotonic saline, it is likely the extended duration reflects the block of ENaC mediated absorption of the salt deposited on aerosol surfaces via aerosolization. Thus, the liquid added to the tracheal surface added in response to aerosolized HS-P308 remained on the tracheal surface for prolonged periods.

Our study provides unique details into the mode of clearance of particles from the trachea. As seen in the Supplementary Movie, particles in the aerosol treated groups continually moved up from deeper in the lungs, into the trachea, suggesting that the insufflation technique dosed lung regions distal to the delivery site. Although we observed particle movement throughout the imaging period, the particulates were not expected to be completely cleared from the imaged airway region over this short imaging period. However, as noted above, the data shows that an aerosol treatment can increase the particle clearance rate when compared to baseline. In all animals, there were particles that remained immobile, likely due to their capture within the periciliary layer and/or persistent adherent mucus. This finding shows that changes in MCT activity produced by rehydration are heterogeneous and that rehydration of adherent mucus may not be rapid. The failure to mobilize all particles suggests that studies must be directed towards understanding this phenomena and how to address it therapeutically. Conversely, there were many particles that moved much more rapidly throughout the imaging period, with a maximum particle MCT rate of 140 mm/min recorded. These high rates typically resulted from cough-like respiratory movements (as suggested by transient spikes in airway pressure; data not shown), or rapid bulk fluid movements, and so were excluded from the statistical analyses.

This study had several limitations. The primary limitation was the small number of mice in the aerosol treatment groups, a direct result of the limited beam-time allocation (a total of 48 hours including experimental setup) available at the SPring-8 synchrotron. In future studies, the effects of MCT altering therapeutics in larger groups of mice, including distinguishing the effects of HS alone (since HS is already used as a CF clinical treatment) from the P308 ENaC blocker

will be studied. Similarly, the effects of using a humidification chamber in the ventilator inspiratory line on the measured MCT will also be quantified. Tracking particles for extended periods (longer than 20 minutes) should also further distinguish the effects of HS and P308. Future studies may also use tracking particles with improved characteristics. The relatively large size of lead particles and the lack of particle surface uniformity likely affected the MCT rates observed. However, the marker particles must be of the appropriate size and X-ray density to be detectable *in vivo* by PCXI, and a dispersion of sizes may mimic real environmental exposures. Finally, it is also possible that the requirement for manual tracking of the deposited particles resulted in observer bias. We minimised this effect by blinding the observer to the treatments. However, we have begun to develop new visual analytical techniques to better address this particle tracking issue.

In summary, this study has shown that the effects of therapeutics thought to restore the MCT rate can be directly quantified using synchrotron PCXI. Moreover, this technique can be readily applied to assessing MCT at any appropriate time-point within lung clearance studies, to test the effects of a variety of pharmaceutical treatments in appropriate mouse model strains. We are continuing our efforts to improve our direct and non-invasive MCT imaging assessment methods to assist our understanding and treatment of respiratory diseases such as CF.

Methods

Ethics statement. Experiments were performed on the BL20XU undulator beamline at the SPring-8 synchrotron radiation facility in Japan, under approvals from the Animal Ethics Committees of SPring-8, the Women’s and Children’s Health Network, and the University of Adelaide.

Imaging setup. The experimental hutch was located in the Biomedical Imaging Centre, 245 metres from the storage ring (see Fig. 1). Monochromatic 25 keV ($\lambda = 0.5\text{\AA}$) X-rays were selected using a standard double-crystal monochromator²⁶. A propagation (sample to detector) distance of ~ 1 m was used as in previous experiments⁴. Images were captured using a high-resolution X-ray converter (SPring-8 BM3) with a sCMOS detector. The converter used a 10 μm thick scintillator ($\text{Lu}_2\text{SiO}_5\text{:Ce}$) to convert X-rays to visible light, which was then directed to the sCMOS sensor using a $\times 10$ microscope objective lens (NA 0.45). The sCMOS detector was a pco.edge (PCO Imaging) with an array size of 2560×2160 pixels and a 6.5×6.5 μm native pixel size. This setup resulted in an effective isotropic pixel size of 0.56 μm and a field of view of 1.43 mm \times 1.2 mm. The incident beam was limited to this size using slits to reduce the radiation dose to the animals. Image capture was synchronised with a fast shutter (Uniblitz XRS6 with VMM-T1 timer unit) and triggered by the ventilator (refer to animal preparation description below) to minimise the dose between exposures. An exposure length of 10 ms was optimal for producing a high SNR without movement blur.

Animal preparation. Mice ($n = 15$, C57Bl/6, weight ~ 18 – 20 grams) were prepared as for previous experiments²⁷. Briefly, mice were anaesthetized with pentobarbital (Somnopenil, Pitman-Moore, Washington Crossing, USA; 100 mg/kg i.p.) and intubated using a fibre-optic illuminated guide wire and a 20 Ga i.v. catheter (Insyte, Becton Dickinson, Utah, USA) as an endotracheal (ET) tube²⁸. The ET tube was inserted into the trachea to a fixed depth of 22.5 mm from the nose tip. This location placed the ET tube tip approximately half way between the epiglottis and the carina to avoid physically perturbing the more distal imaging region. The fur around the imaging area was removed using surgical clippers (CareFusion, San Diego, USA; Neuro blade) followed by depilatory cream (Nair, Church & Dwight, Australia). After intubation a small quantity (less than 0.001 g) of lead dust was delivered to the trachea and lungs using a Dry Powder Insufflator™ Model DP-4M (Penn-Century, Wyndmoor, PA, USA). The particle size distribution was as previously described⁴. Due to high variability in the output (particle mass) of the first actuation of the air pump, the first output was discarded and the second actuation was used to deliver the sample to the airways. The insufflator was thoroughly cleaned with compressed air between deliveries to remove any residual particles prior to reloading.

Mice were tethered to an imaging board with their dorsal incisors hooked over a stainless-steel wire loop and the limbs, and their shoulders and torso were taped to the board to minimise body movements that interfere with high-resolution imaging. The imaging board was mounted on the hutch sample stage so that the mouse was oriented supine and the X-ray beam passed laterally through the mouse trachea, approximately five cartilage rings distal to the tip of the ET tube. Anaesthesia was maintained throughout the experiment by constant pentobarbital infusion (0.1 mg/kg/sec) via an indwelling i.p. needle attached to a micro-syringe pump (UltraMicroPump III and Micro4 controller, World Precision Instruments, Florida, USA). The ET tube was attached to a flexiVent small animal ventilator (SCIREQ, Montreal, Canada), and ventilation was set at 120 breaths/min, a tidal volume of



15 ml/kg (minute ventilation of approximately 1.8 ml/g), and ~ 3 cmH₂O of PEEP. The flexiVent provided a trigger to capture a single image during each end-expiratory pause. Body temperature was maintained using an infrared heat lamp.

Aerosol treatment and imaging. Mice were randomly assigned to one of three groups; a no treatment control group (No Rx Control, n = 5); an isotonic saline control group (n = 4); or the treatment group (n = 3). Mice in the treatment group (HS-P308) received compound P308 (Parion Sciences, Durham, NC, USA), a potent and long acting epithelial sodium channel (ENaC) blocker, at a concentration of 1 mM, in 7% HS to produce the maximal rehydrating effect. One image was captured per breath (2 Hz) for a 30 second period every 2 min (see Fig. 2) to reduce radiation dose and maintain shutter performance. After two imaging periods were obtained to calculate the baseline MCT rate prior to treatment, the aerosol was delivered for 2.5 min using an Aeronex nebuliser (Aerogen, Ireland) designed to produce a 4–6 μ m volume median diameter aerosol. The Aeronex was attached to the ventilator inspiratory line, and the flexiVent controlled aerosol delivery to occur at a 50% duty cycle during inspiration only. Imaging continued for a further ~ 20 minutes (a total of 11 time-points) before mice were humanely killed via Nembutal overdose without waking from anaesthesia.

Post experimental analyses. All images were flat-field and dark-current corrected (Matlab R2012b, The Mathworks, Natick, MA, USA). Changes in image brightness produced by the inherent instability of the X-ray beam (manifested primarily as flicker caused by rapid changes in the vertical position of the beam over time) were minimised using a flicker-reduction algorithm that normalised the intensity of each row of pixels in the image.

Individual particle MCT rates were quantified using a Matlab program that presented an observer with 10 frames (from one imaging period) over which particle motion was to be tracked. For the treatment groups the 10 frames were sequential (i.e. every breath). For the control group and all baseline measurements every fifth frame was used to improve tracking accuracy at slow particle MCT rates. The observer was then asked to manually track the location of a chosen particle in each of those 10 frames. The 10 frame sequence was then presented again, this time with the location of the previously tracked particle(s) shown, and the observer was asked to track another particle. This process was repeated until a maximum of 50 particles were tracked, or no further moving particles could be identified in the sequence. The analysis then proceeded to the next imaging period (see Fig. 2), until all 11 periods were analysed. This whole cycle was repeated for each animal, with the observer blinded to any information that would identify the treatment that an animal had received, thereby preventing observer bias.

The distance that each particle moved between each of the 10 frames was calculated in pixels and converted to millimetres based on the size of the field of view. The MCT rate was then calculated (in mm/min) based on the time between analysis frames. Particles moving faster than 15 mm/min (chosen based on previous studies^{11,12}) were excluded from further analysis because these likely resulted from ‘cough-like’ movements or rapid bulk fluid movements. A mean MCT rate was calculated for each time-point in every animal. Statistical analyses were performed using GraphPad Prism 5. Data were tested for normality, statistical significance was set at $p = 0.05$ and power = 0.80 and MCT rates were analysed by two way RM-ANOVA with Bonferroni multiple comparisons. MCT rates are presented as mean and standard error of the mean ($\bar{X} \pm SE$).

Images were created to show the motion of tracked particles at each time-point. A supplementary movie file (.avi format) was also assembled from the processed post-deposition images to compare particulate behaviour on the tracheal airway surface in the three groups. The movie frame rate was set to 5 \times normal speed, was encoded using the Xvid codec and can be played using the free VLC Media Player (available at <http://www.videolan.org/vlc/>).

- Boucher, R. C. New concepts of the pathogenesis of cystic fibrosis lung disease. *Eur Respir J* **23**, 146–158, doi:10.1183/09031936.03.00057003 (2004).
- Stocker, A. *et al.* Single-dose lentiviral gene transfer for lifetime airway gene expression. *J Gene Med* **11**, 861–867, doi:10.1002/jgm.1368 (2009).
- Limberis, M., Anson, D. S., Fuller, M. & Parsons, D. W. Recovery of airway cystic fibrosis transmembrane conductance regulator function in mice with cystic fibrosis after single-dose lentivirus-mediated gene transfer. *Hum Gene Ther* **13**, 2112–2112, doi:10.1089/10430340260355365 (2002).
- Donnelley, M., Morgan, K., Siu, K. K. W. & Parsons, D. W. Dry deposition of pollutant and marker particles onto live mouse airway surfaces enhances monitoring of individual particle mucociliary transit behaviour. *J Synchrotron Radiat* **19**, 551–558, doi:10.1107/S0909049512018250 (2012).
- Donnelley, M. *et al.* A new technique to examine individual particle and fibre deposition and transit behaviour on live mouse trachea. *J Synchrotron Radiat* **17**, 719–729, doi:10.1107/S0909049510028451 (2010).
- Donnelley, M. *et al.* Real-time non-invasive detection of inhalable particulates delivered into live mouse airways. **16**, 553–561, doi:10.1107/S0909049509012618 (2009).
- Grubb, B. R., Jones, J. H. & Boucher, R. C. Mucociliary transport determined by in vivo microdialysis in the airways of normal and CF mice. *Am J Physiol Lung Cell Mol Physiol* **286**, L588–595, doi:10.1152/ajplung.00302.2003 (2004).
- Donaldson, S. H., Corcoran, T. E., Laube, B. L. & Bennett, W. D. Mucociliary clearance as an outcome measure for cystic fibrosis clinical research. *Proc Am Thorac Soc* **4**, 399–405, doi:10.1513/pats.200703-042BR (2007).
- Livraghi, A. & Randell, S. H. Cystic fibrosis and other respiratory diseases of impaired mucus clearance. *Toxicologic pathology* **35**, 116–129, doi:10.1080/10926230601060025 (2007).
- Hua, X. Y. *et al.* Noninvasive real-time measurement of nasal mucociliary clearance in mice by pinhole gamma scintigraphy. *J Appl Physiol* **108**, 189–196, doi:10.1152/jappphysiol.00669.2009 (2010).
- Cooper, J. L., Quinton, P. M. & Ballard, S. T. Mucociliary transport in porcine trachea: differential effects of inhibiting chloride and bicarbonate secretion. *Am J Physiol Lung C* **304**, L184–L190, doi:10.1152/ajplung.00143.2012 (2013).
- Ballard, S. T., Parker, J. C. & Hamm, C. R. Restoration of mucociliary transport in the fluid-depleted trachea by surface-active instillates. *Am J Resp Cell Mol* **34**, 500–504, doi:10.1165/rcmb.2005-0214OC (2006).
- Snigirev, A., Snigireva, I., Kohn, V., Kuznetsov, S. & Schelokov, I. On the possibilities of x-ray phase contrast microimaging by coherent high-energy synchrotron radiation. *Rev Sci Instrum* **66**, 5486–5492, doi:10.1063/1.1146073 (1995).
- Cloetens, P., Barrett, R., Baruchel, J., Guigay, J. P. & Schlenker, M. Phase objects in synchrotron radiation hard X-ray imaging. *J Phys D Appl Phys* **29**, 133–146, doi:10.1088/0022-3727/29/1/023 (1996).
- Wilkins, S. W., Gureyev, T. E., Gao, D., Pogany, A. & Stevenson, A. W. Phase-contrast imaging using polychromatic hard X-rays. *Nature* **384**, 335–338, doi:10.1038/384335a0 (1996).
- Parsons, D. W. *et al.* High-resolution visualization of airspace structures in intact mice via synchrotron phase-contrast X-ray imaging (PCXI). *J Anat* **213**, 217–227, doi:10.1111/j.1469-7580.2008.00950.x (2008).
- Siu, K. K. W. *et al.* Phase contrast X-ray imaging for the non-invasive detection of airway surfaces and lumen characteristics in mouse models of airway disease. *Eur J Radiol* **68**, S22–S26, doi:10.1016/j.ejrad.2008.04.029 (2008).
- Donnelley, M., Morgan, K., Siu, K. & Parsons, D. Variability of in vivo fluid dose distribution in mouse airways is visualized by high-speed synchrotron x-ray imaging. *J Aerosol Med Pulm D* **26**, 1–10, doi:10.1089/jamp.2012.1007 (2012).
- Donnelley, M., Siu, K., Jamison, A. & Parsons, D. Synchrotron phase contrast X-ray imaging reveals fluid dosing dynamics in mouse airways. *Gene Ther* **19**, 8–14, doi:10.1038/gt.2011.80 (2012).
- Robinson, M. *et al.* Effect of increasing doses of hypertonic saline on mucociliary clearance in patients with cystic fibrosis. *Thorax* **52**, 900–903, doi:10.1136/thx.52.10.900 (1997).
- Button, B., Okada, S. F., Frederick, C. B., Thelin, W. R. & Boucher, R. C. Mechanosensitive ATP release maintains proper mucus hydration of airways. *Science signaling* **6**, ra46, doi:10.1126/scisignal.2003755 (2013).
- Tarran, R., Trout, L., Donaldson, S. H. & Boucher, R. C. Soluble mediators, not cilia, determine airway surface liquid volume in normal and cystic fibrosis superficial airway epithelia. *The Journal of general physiology* **127**, 591–604, doi:10.1085/jgp.200509468 (2006).
- Donaldson, S. H. *et al.* Mucus clearance and lung function in cystic fibrosis with hypertonic saline. *New Engl J Med* **354**, 241–250, doi:10.1056/Nejm043891 (2006).
- Hirsh, A. J. *et al.* Pharmacological properties of N-(3,5-diamino-6-chloropyrazine-2-carbonyl)-N'-4-[4-(2,3-dihydroxypropoxy)phenyl]butyl-guanidine methanesulfonate (552-02), a novel epithelial sodium channel blocker with potential clinical efficacy for cystic fibrosis lung disease. *J Pharmacol Exp Ther* **325**, 77–88, doi:10.1124/jpet.107.130443 (2008).
- JL, G. & B, B. An In Vitro Study of the Kinetics of Hypertonic Saline on ASL Height. *Pediatr Pulm* **45**:S33, 291.
- Yabashi, M. *et al.* SPring-8 standard x-ray monochromators. *Proc. SPIE* **3773**, 2–13, doi:10.1117/12.370098 (1999).
- Donnelley, M., Parsons, D., Morgan, K. & Siu, K. Animals In Synchrotrons: Overcoming Challenges For High-Resolution, Live, Small-Animal Imaging. *AIP Conf Proc* **1266**, doi:10.1063/1.3478192 (2010).
- Hamacher, J. *et al.* Microscopic wire guide-based orotracheal mouse intubation: description, evaluation and comparison with transillumination. *Lab Anim* **42**, 222–230, doi:10.1258/la.2007.006068 (2008).

Acknowledgments

Studies supported by the Women’s and Children’s Hospital Foundation, NHMRC Australia (Project 626863) and philanthropic donors via the Cure4CF Foundation (www.cure4cf.org). The synchrotron radiation experiments were performed on the BL20XU beamline at SPring-8, with the approval of the Japan Synchrotron Radiation Institute (JASRI) under proposal number 2011B1371. We thank Prof Naoto Yagi, Dr Kentaro Uesugi, Dr Yoshio Suzuki and Dr Akihisa Takeuchi for their assistance with experimental setup. RB provided the P308 compound used in this study. MD is supported by a MS McLeod Fellowship, KM by an ARC DECRA, AF by a NHMRC CDF, and NF by a MS McLeod PhD Scholarship. All authors were supported by the Australian Synchrotron International Synchrotron Access Program (ISAP). The ISAP is an initiative of the Australian Government being conducted as part of the National Collaborative Research Infrastructure Strategy. The funders had no role in study design, data collection and analysis, decision to publish, or preparation of the manuscript.



Author contributions

M.D. and D.P. conceived and designed the experiments. M.D., K.M., K.S., N.F., C.S., A.F. and D.P. performed the experiments. M.D., R.B. and D.P. analysed the data and wrote the manuscript. All authors reviewed and edited the manuscript.

Additional information

Supplementary information accompanies this paper at <http://www.nature.com/scientificreports>

Competing financial interests: RCB is a co-founder and Chairman of the Board of Parion Sciences Inc. There are no other competing financial interests.

How to cite this article: Donnelley, M. *et al.* Non-invasive airway health assessment: Synchrotron imaging reveals effects of rehydrating treatments on mucociliary transit in-vivo. *Sci. Rep.* **4**, 3689; DOI:10.1038/srep03689 (2014).



This work is licensed under a Creative Commons Attribution-NonCommercial-NoDerivs 3.0 Unported license. To view a copy of this license, visit <http://creativecommons.org/licenses/by-nc-nd/3.0>



DOI: 10.1038/srep05361

SUBJECT AREAS:
PRE-CLINICAL STUDIES
BIOMEDICAL ENGINEERING
ANATOMY

CORRIGENDUM: Non-invasive airway health assessment: Synchrotron imaging reveals effects of rehydrating treatments on mucociliary transit in-vivo

Martin Donnelley, Kaye S. Morgan, Karen K. W. Siu, Nigel R. Farrow, Charlene S. Stahr, Richard C. Boucher, Andreas Fouras & David W. Parsons

SCIENTIFIC REPORTS:
4 : 3689
DOI: 10.1038/srep03689

The Acknowledgements section in this Article is incomplete; it should also include the following NIH grant number:
"NHLBI P01-HL110873"

Published:
14 January 2014

Updated:
16 July 2014